

**Probing the GRB prompt emission mechanism,
magnetic field geometry, and jet structure with
linear polarization**

Ramandeep Gill

The Open University of Israel
Institute for Theoretical Physics, Frankfurt

Collaborators:

Jonathan Granot & Pawan Kumar

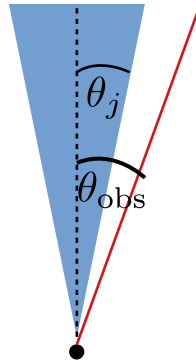
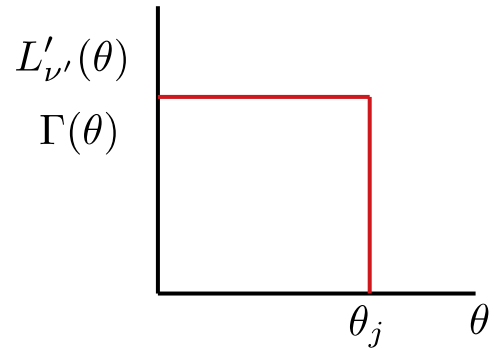
Outline of the talk

- **Structured jets**
 - Dependence of fluence on the viewing angle
 - Limitation to small viewing angles due to compactness
- **Polarization from different radiation processes: Top-hat jet Vs structured jet**
 - **Synchrotron emission**
 - Temporal evolution
 - Different B-field configurations
 - **Non-dissipative photospheric emission**
 - **Compton drag**
- **Change in net polarization when integrating over multiple pulses**
- **Monte-Carlo simulation of polarized emission from a large sample of GRBs**
 - What can we say about the B-field structure?
 - Can we infer anything about the jet structure?

Structured jets

Jet geometry

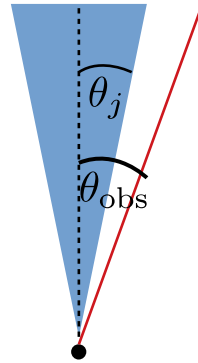
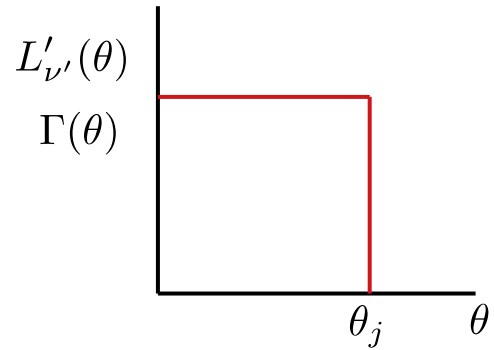
Top-hat jet



A uniform jet with a sharp edge

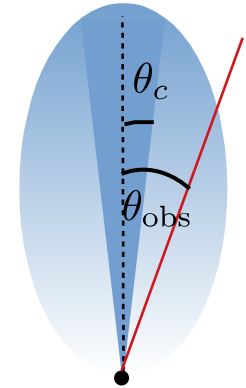
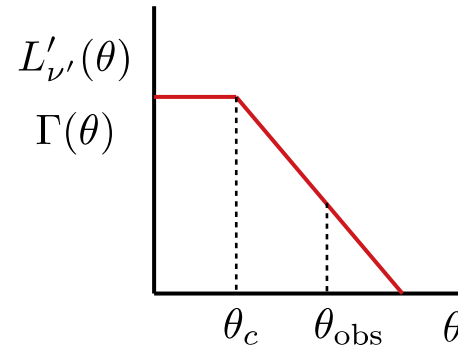
Jet geometry

Top-hat jet



A uniform jet with a sharp edge

Structured jet



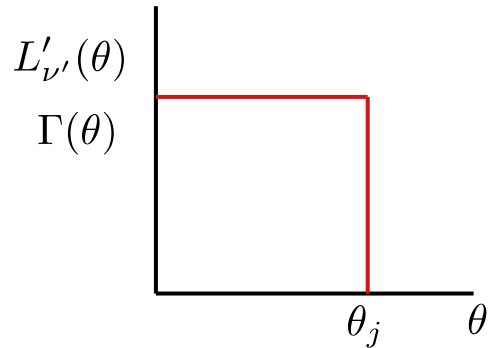
$$L'_{\nu'} \propto \Theta^{-a}$$

$$\Gamma(\theta) \propto \Theta^{-b}$$

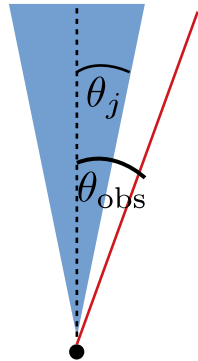
$$\Theta = \sqrt{1 + \left(\frac{\theta}{\theta_c}\right)^2}$$

Jet geometry

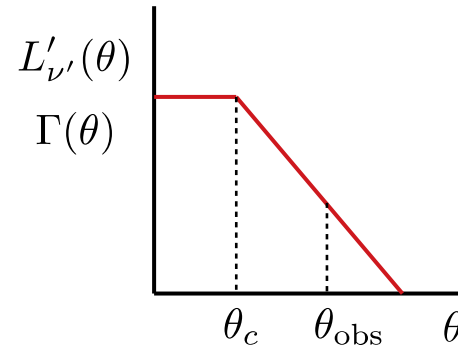
Top-hat jet



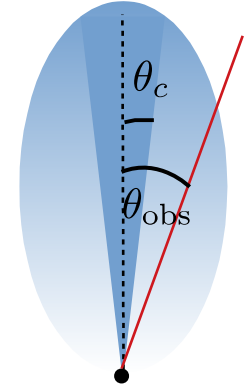
A uniform jet with a sharp edge



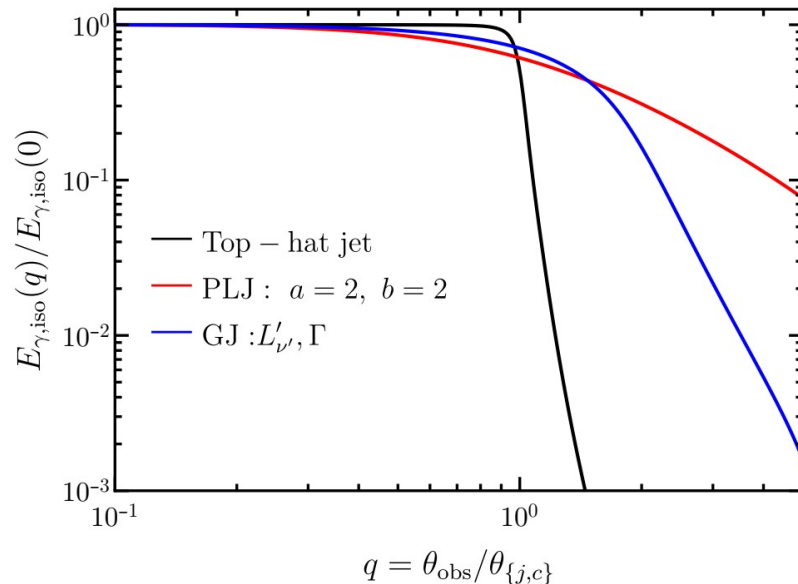
Structured jet



$$L'_{\nu} \propto \Theta^{-a} \quad \Gamma(\theta) \propto \Theta^{-b} \quad \Theta = \sqrt{1 + \left(\frac{\theta}{\theta_c}\right)^2}$$



Off-axis to on-axis fluence ratio



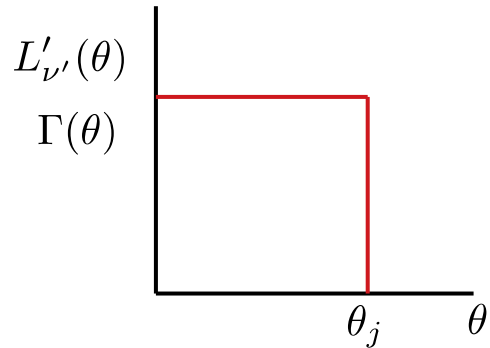
$$E_{\gamma, \text{iso}} = \frac{4\pi d_L^2}{(1+z)} S_{\gamma}$$

$$S_{\gamma} = \int dt_{\text{obs}} \int_{\nu_1}^{\nu_2} d\nu F_{\nu}(t_{\text{obs}})$$

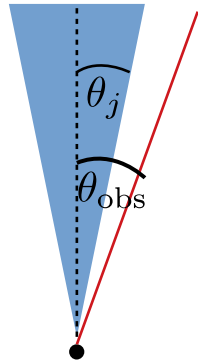
- Fluence is suppressed for off-axis observers, which makes it hard to detect distant off-axis GRBs. (Granot+02; Yamazaki+03; Eichler & Levinson 04; Salafia+15)
- Structured jets are visible over much larger angular scales than top-hat jets.

Jet geometry

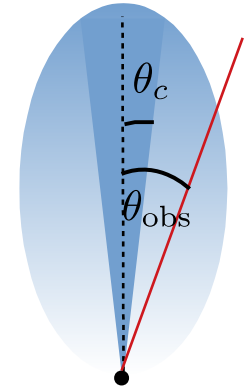
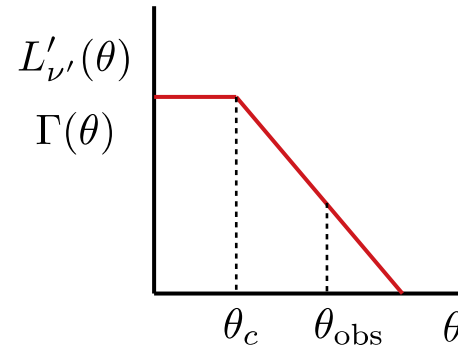
Top-hat jet



A uniform jet with a sharp edge



Structured jet



$$L'_{\nu} \propto \Theta^{-a} \quad \Gamma(\theta) \propto \Theta^{-b} \quad \Theta = \sqrt{1 + \left(\frac{\theta}{\theta_c}\right)^2}$$

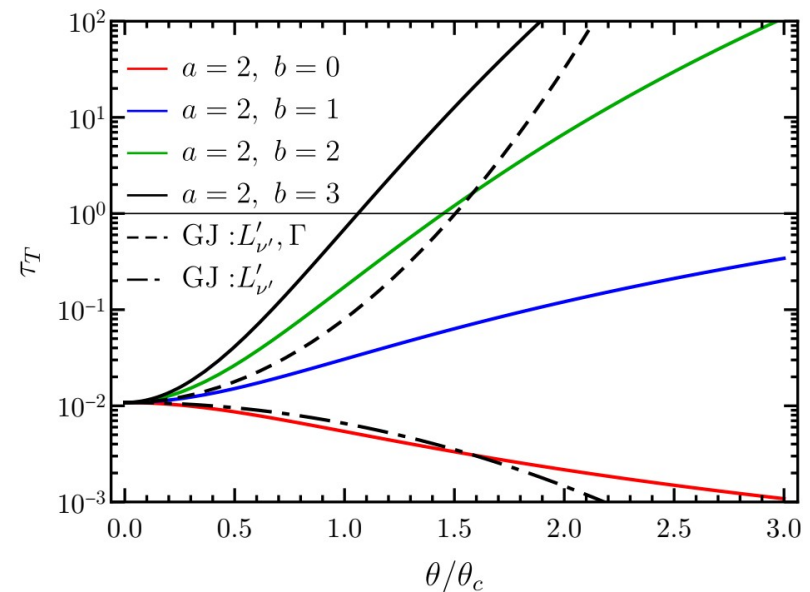
- Pair-production and its effect on the spectrum becomes important when the compactness of the flow is high.

$$\ell'_{\gamma} = \sigma_T \frac{U'_{\gamma}}{m_e c^2} \frac{R}{\Gamma} = f_{\gamma\gamma}^{-1} \tau_T$$

- High Thomson scattering optical depth due to pairs can suppress γ -ray emission

$$\tau_T \approx \epsilon_{\gamma} f_{\gamma\gamma} \frac{3\sigma_T}{8m_e c^4} \frac{L_k(\theta)}{\Gamma^5 t_{v,z}}$$

Compactness constraints



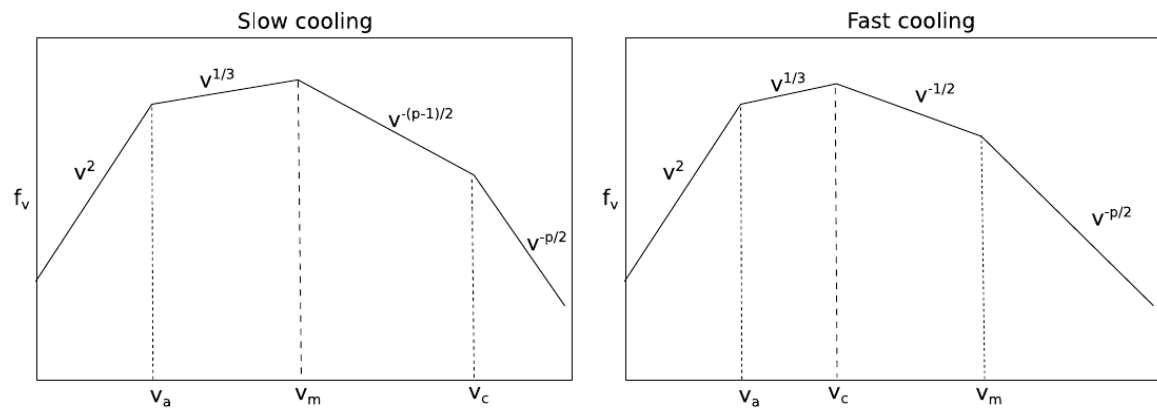
Polarization from different radiation processes

Synchrotron emission

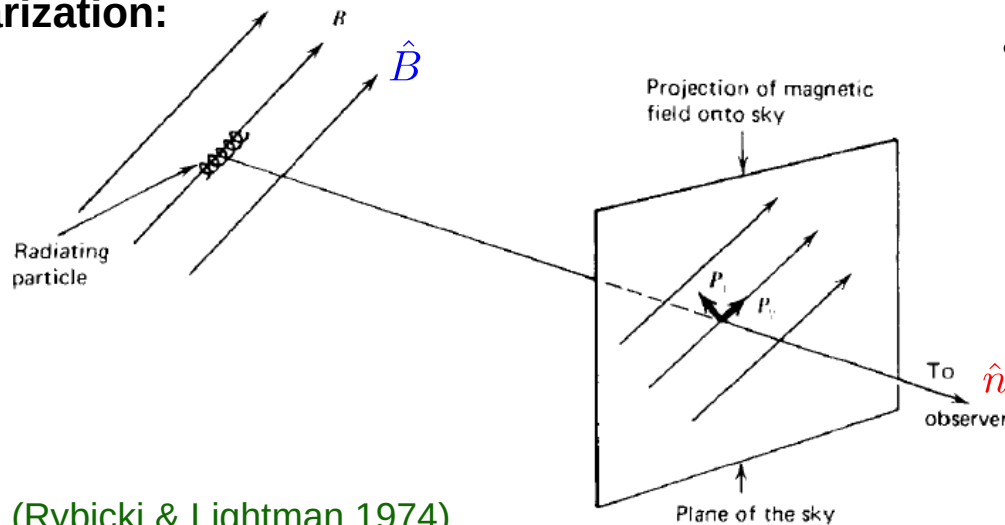
- Relativistic particles (e^- or e^\pm) gyrate around magnetic field lines and emit synchrotron photons.
- Energy distribution of particles follow a power law: $n_e(\gamma_e) \propto \gamma_e^{-p}$ $\gamma_m < \gamma_e < \gamma_M$

Spectrum: $F_\nu \propto \nu^{-\alpha}$

(Sari+98; Granot & Sari 02)



Polarization:



(Rybicki & Lightman 1974)

- Synchrotron emission is generally partially **linearly polarized**

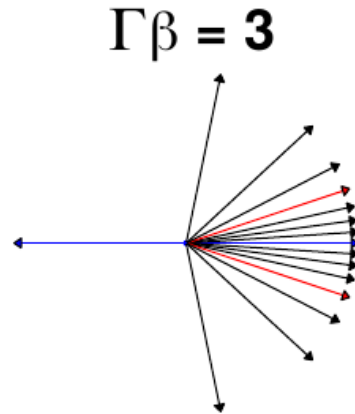
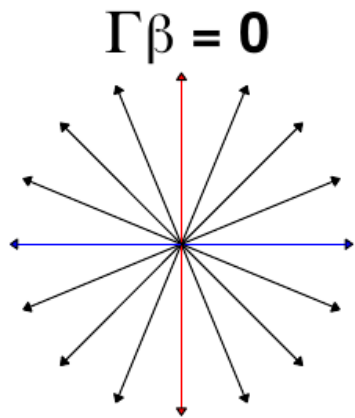
$$\hat{\Pi} = \hat{n} \times \hat{B}$$

$$\Pi_{\max} = \frac{\alpha + 1}{\alpha + 5/3} \xrightarrow[\text{cooling}]{\text{slow}} \frac{p + 1}{p + 7/3}$$

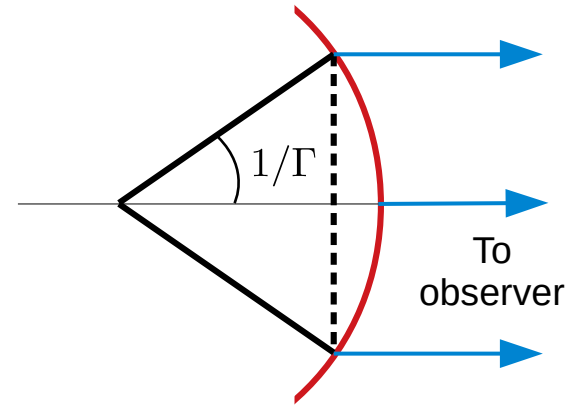
$$0.5 \leq \Pi_{\max} \leq 0.75$$

Synchrotron emission – random B-field

Aberration of light in a relativistic outflow



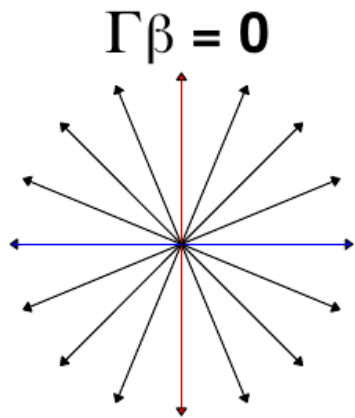
(Granot & Ramirez-Ruiz 2011)



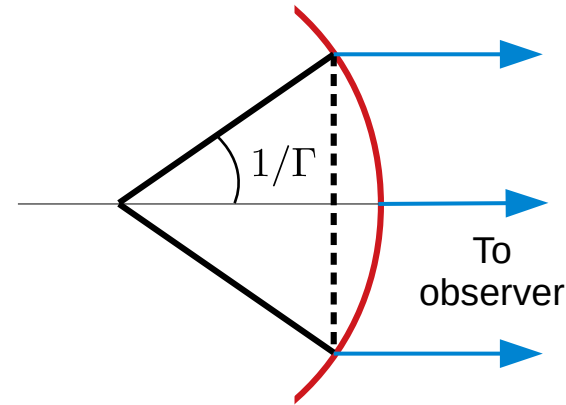
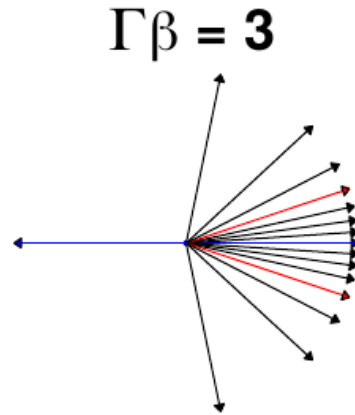
$$\xi \equiv (\Gamma\theta)^2$$

Synchrotron emission – random B-field

Aberration of light in a relativistic outflow

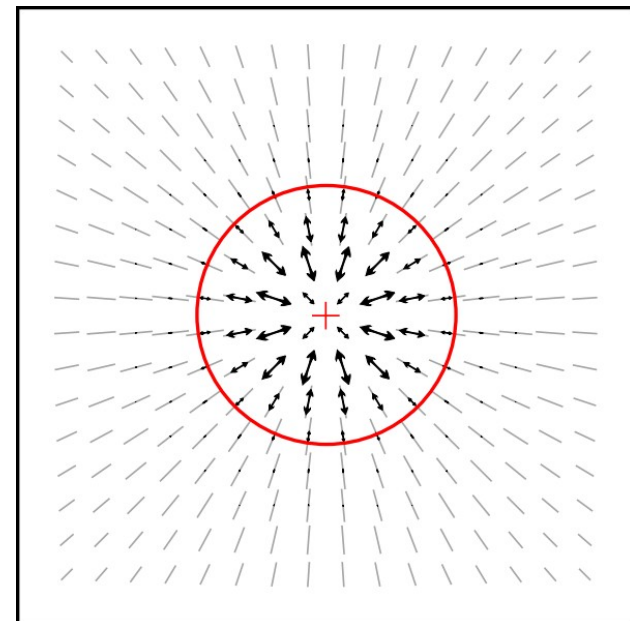


(Granot & Ramirez-Ruiz 2011)



$$\xi \equiv (\Gamma\theta)^2$$

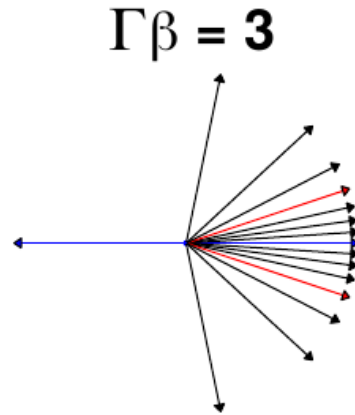
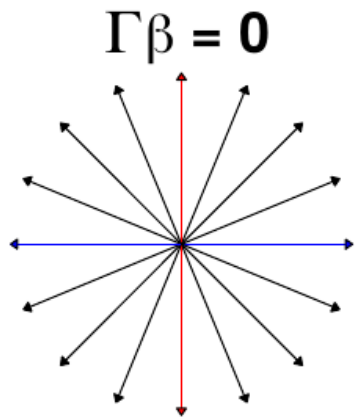
- Greater degree of symmetry in the polarization vectors, when observed over the entire GRB image, leads to smaller degree of **net** polarization



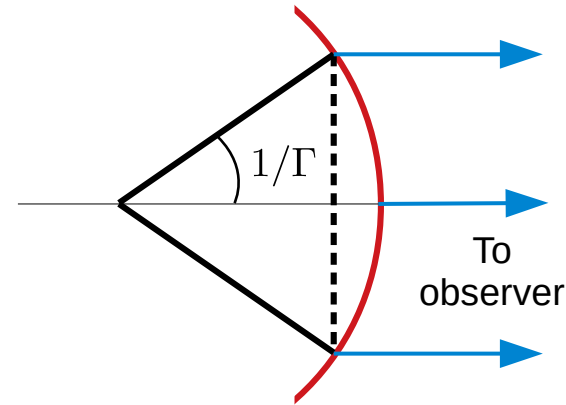
Random B-field (B_{\perp})

Synchrotron emission – random B-field

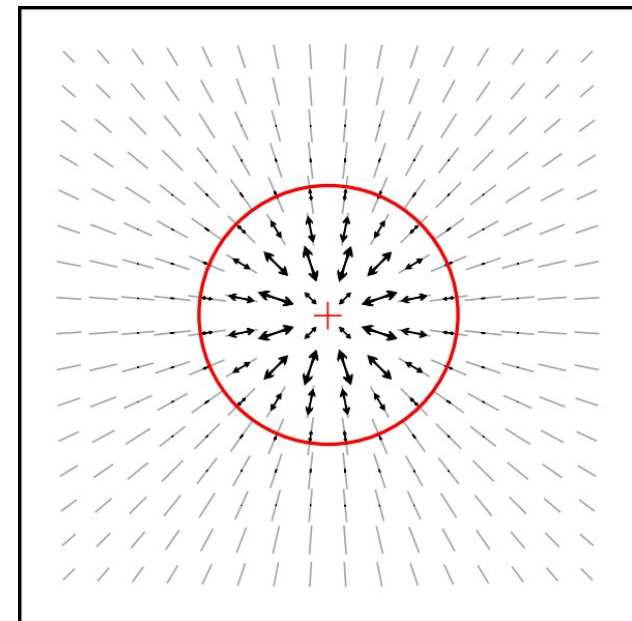
Aberration of light in a relativistic outflow



(Granot & Ramirez-Ruiz 2011)



- Greater degree of symmetry in the polarization vectors, when observed over the entire GRB image, leads to smaller degree of **net** polarization
- One way to **break the symmetry** is by having the line-of-sight close to the jet edge (in a top-hat jet), which will not cancel all the polarization. (Waxman 03)

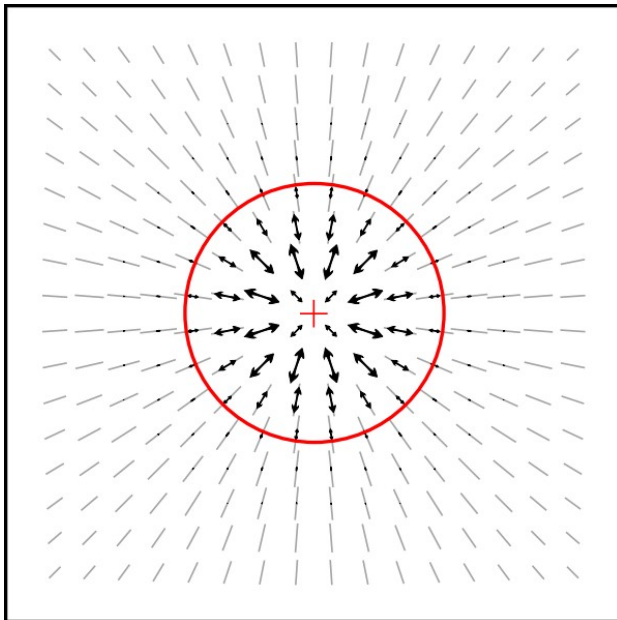


Random B-field (B_{\perp})

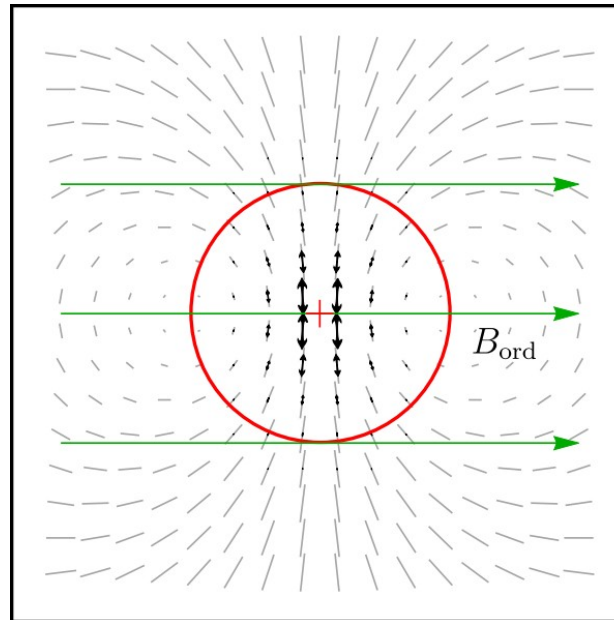
Synchrotron emission – B-field structure

- Large scale B-field breaks the symmetry and yields higher levels of polarization.

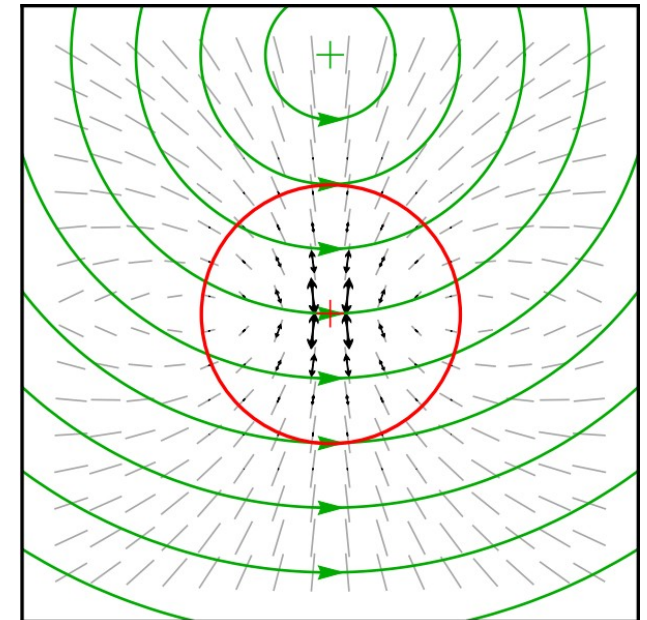
(Granot & Ramirez-Ruiz 11; Gill+18, in prep.)



Random B-field (B_{\perp})



Ordered B-field

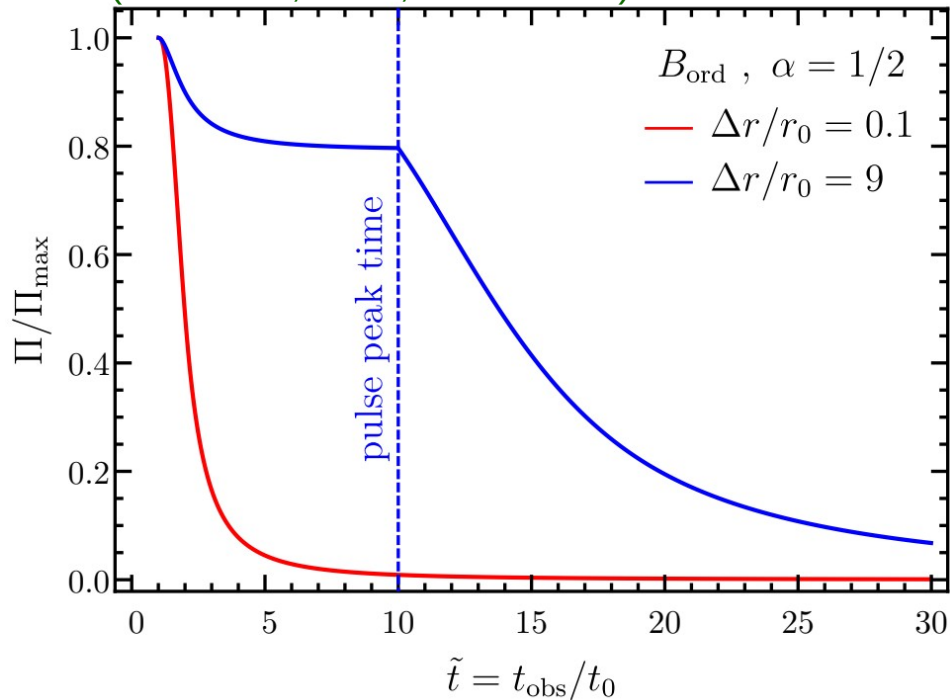


Toroidal B-field (B_{tor})

- Random B-field in the plane transverse to the radial vector
- We also consider B-field parallel to radial vector B_{\parallel}

Temporal evolution of polarization over a single pulse

(see Nakar, Piran, Waxman 03)



- Consider an **ordered B-field** in the entire observed region and a **relativistic spherical shell** emitting between radii

$$r = r_0 \quad \text{and} \quad r = r_0 + \Delta r$$

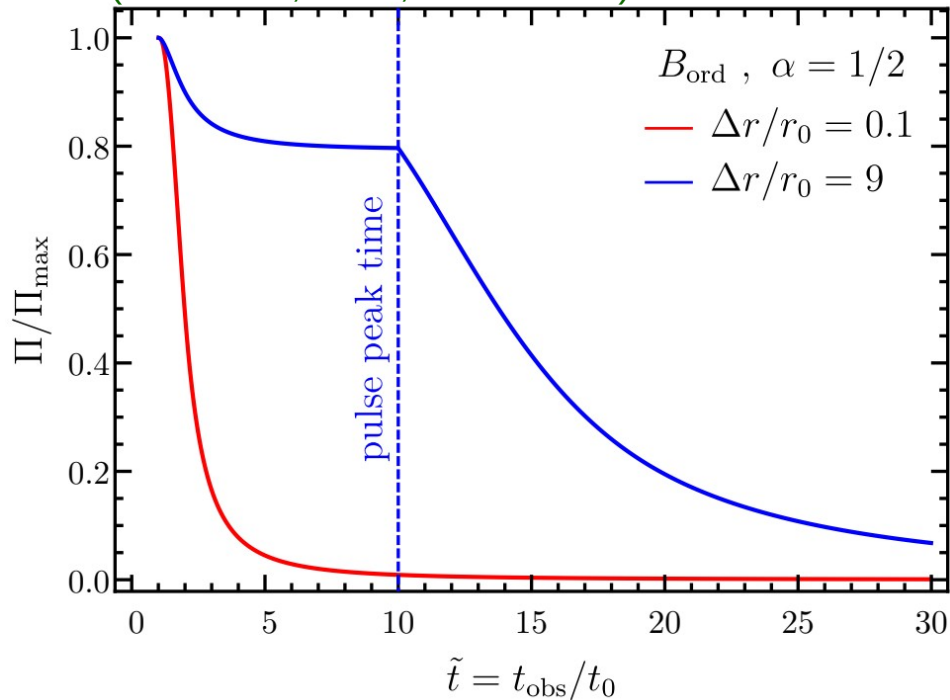
- Emission arrives over two timescales:

Radial time: $\frac{t_{\text{obs},r}}{(1+z)} = \frac{\Delta r}{2\Gamma^2 c}$

Angular time: $\frac{t_{\text{obs},\theta}}{(1+z)} = \frac{r_0}{2\Gamma^2 c}$

Temporal evolution of polarization over a single pulse

(see Nakar, Piran, Waxman 03)



Integration over the entire pulse

- **Simplifying assumption:** Synchrotron emissivity and properties of the emission region do not vary with radius
- This is equivalent to delta-function emission in radius, and the total polarization is obtained by integrating over large angular scales around the LOS:

$$\tilde{\xi}_{\text{max}} = (\Gamma \tilde{\theta}_{\text{max}})^2 > 1$$

- Consider an **ordered B-field** in the entire observed region and a **relativistic spherical shell** emitting between radii

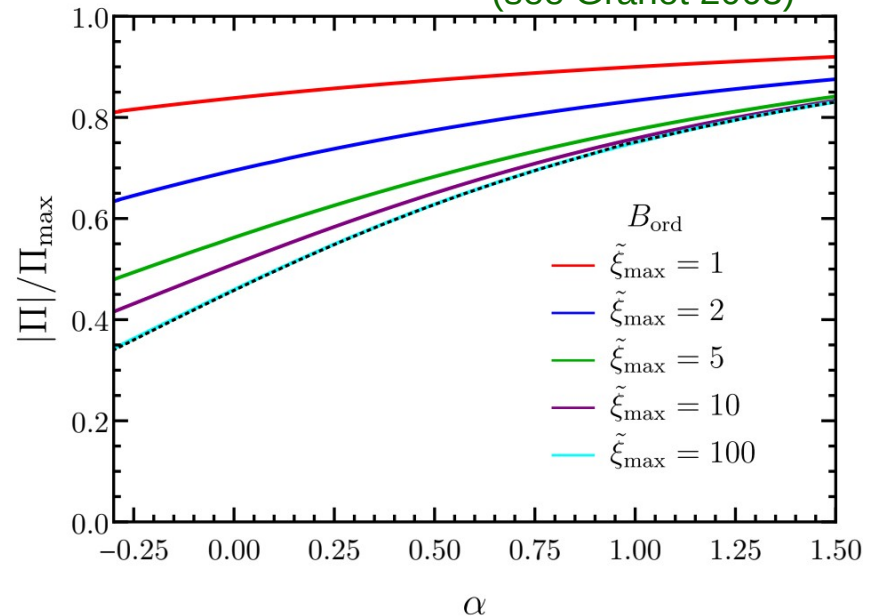
$$r = r_0 \quad \text{and} \quad r = r_0 + \Delta r$$

- Emission arrives over two timescales:

Radial time: $\frac{t_{\text{obs},r}}{(1+z)} = \frac{\Delta r}{2\Gamma^2 c}$

Angular time: $\frac{t_{\text{obs},\theta}}{(1+z)} = \frac{r_0}{2\Gamma^2 c}$

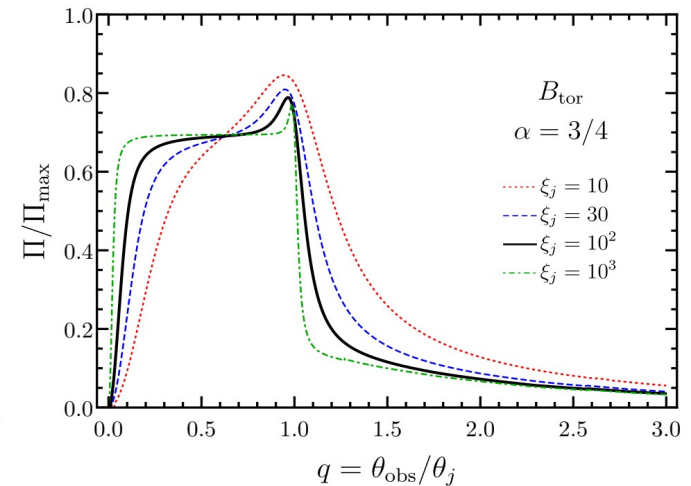
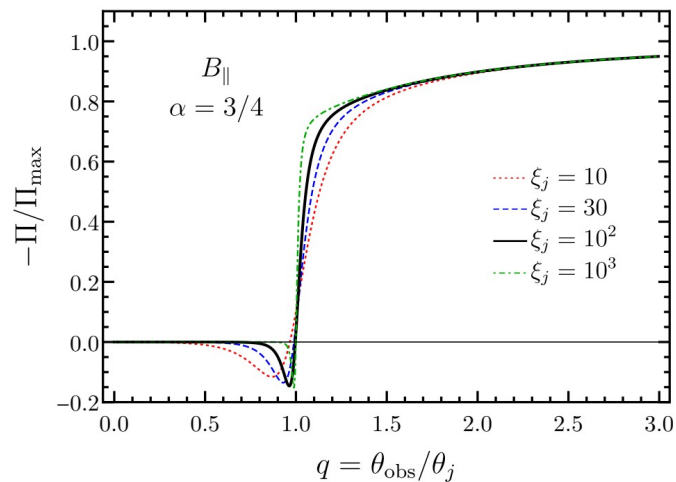
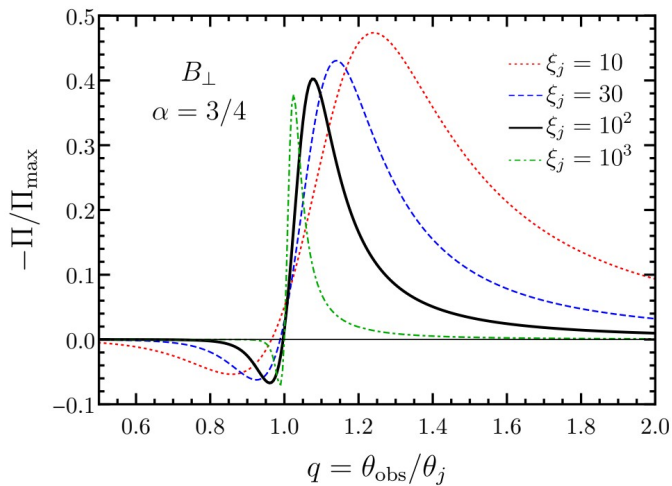
(see Granot 2003)



Synchrotron emission – Polarization

Top-hat jet

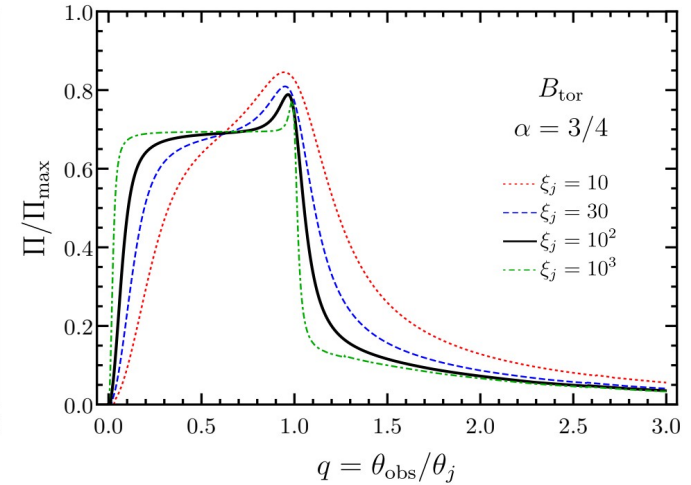
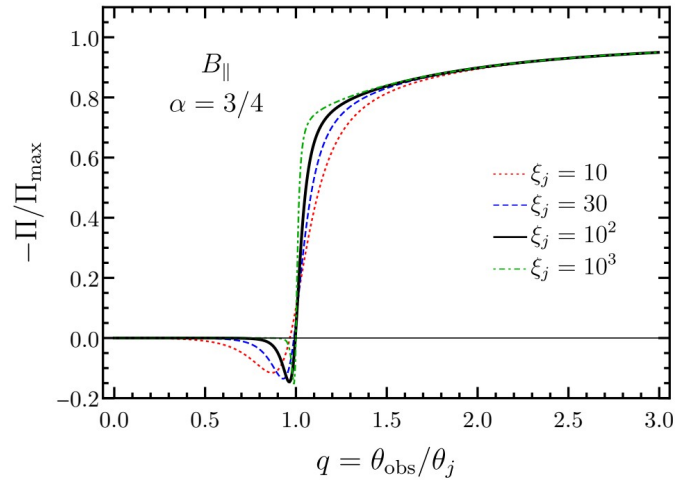
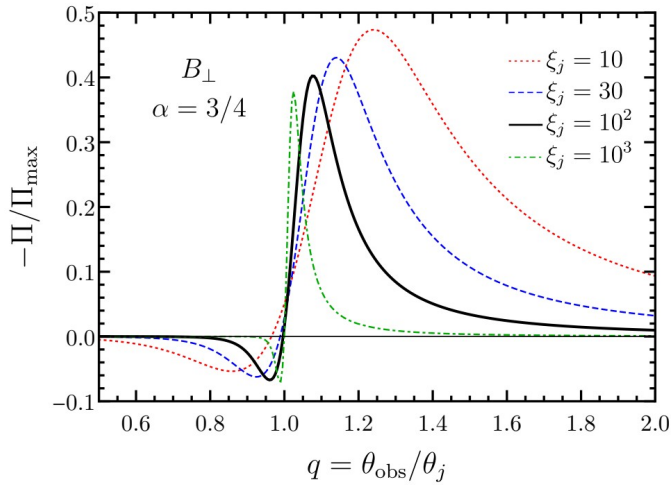
(Granot 03; Granot & Taylor 05; Gill+18, in prep.)



Synchrotron emission – Polarization

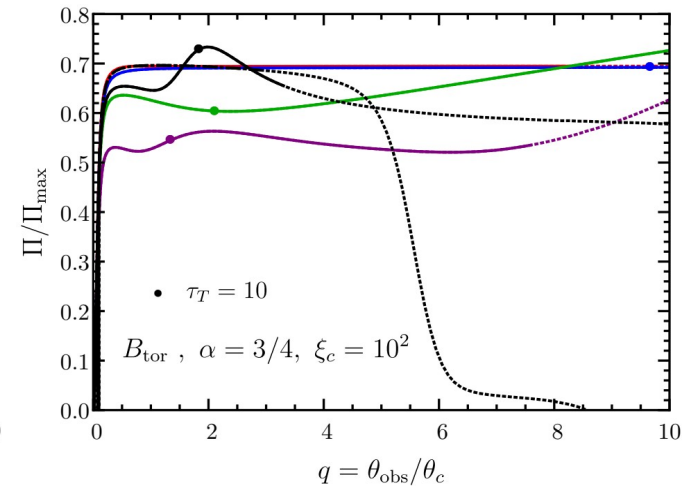
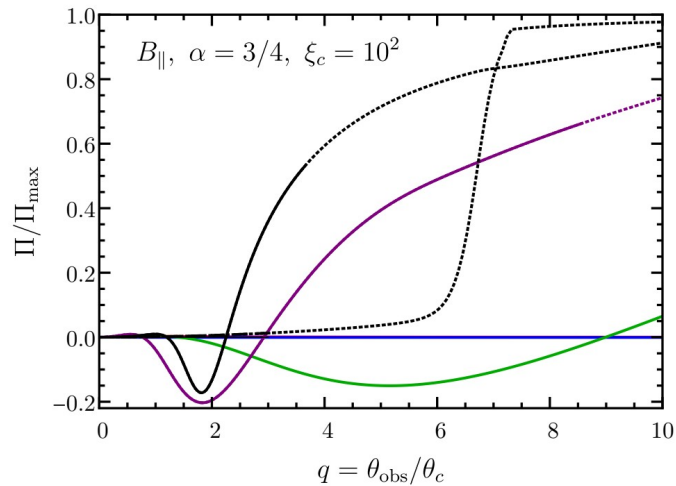
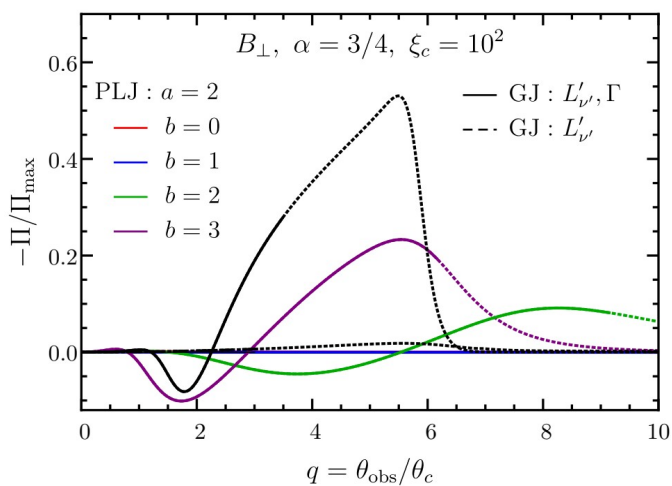
Top-hat jet

(Granot 03; Granot & Taylor 05; Gill+18, in prep.)



Structured jet

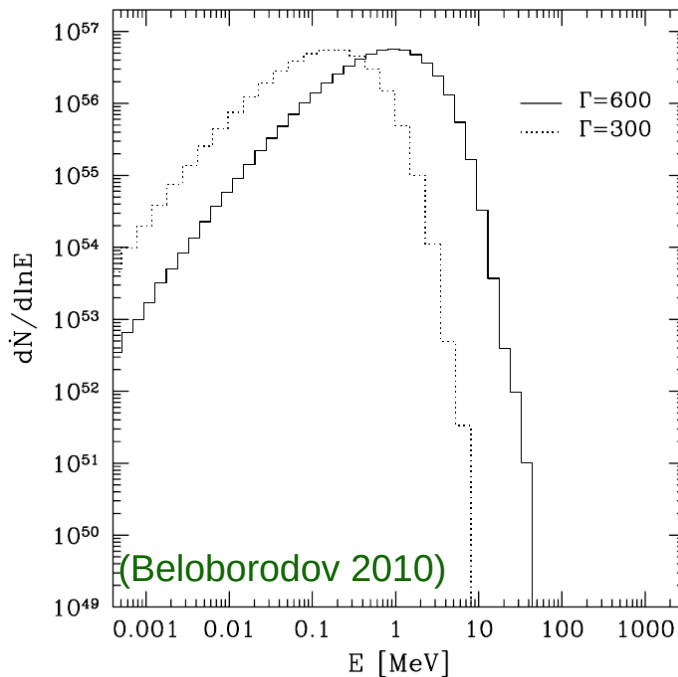
(Gill+18, in prep.)



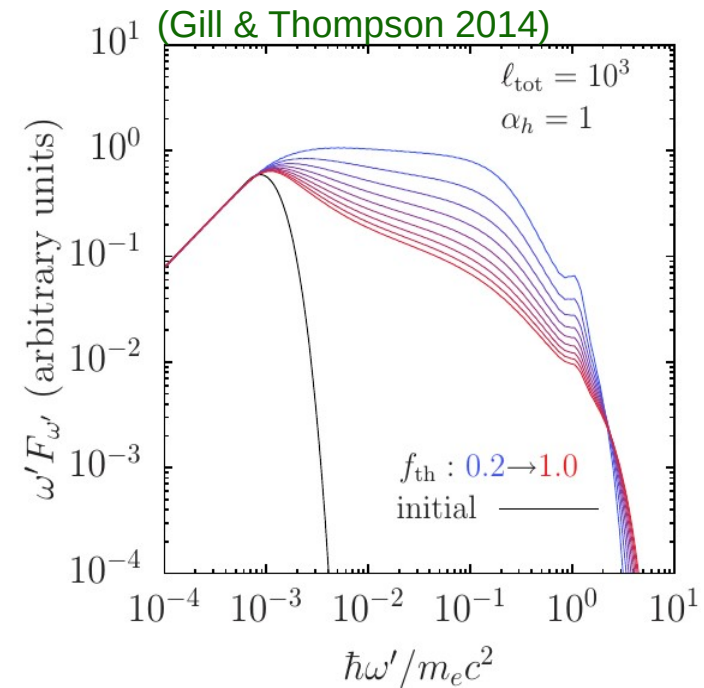
Photospheric emission

- Close to the central engine, the flow is launched highly optically thick to pair-production where it is thermalized via Comptonization.
- Adiabatically cooled thermal radiation is released at the photosphere. (Goodman 86, Paczynski 86)
- Dissipation below and above the photosphere produces the non-thermal GRB spectrum. (Thompson 94; Eichler & Levinson 00; Meszaros & Rees 05; Lazzati+09; Peer & Ryde 11; Begue+13; Thompson & Gill 14; Gill & Thompson 14; Vurm & Beloborodov 16)

Non-dissipative outflow



Heated outflow



- Spectrum shown in the comoving frame, with different levels of heating.

Non-dissipative photospheric emission - Polarization

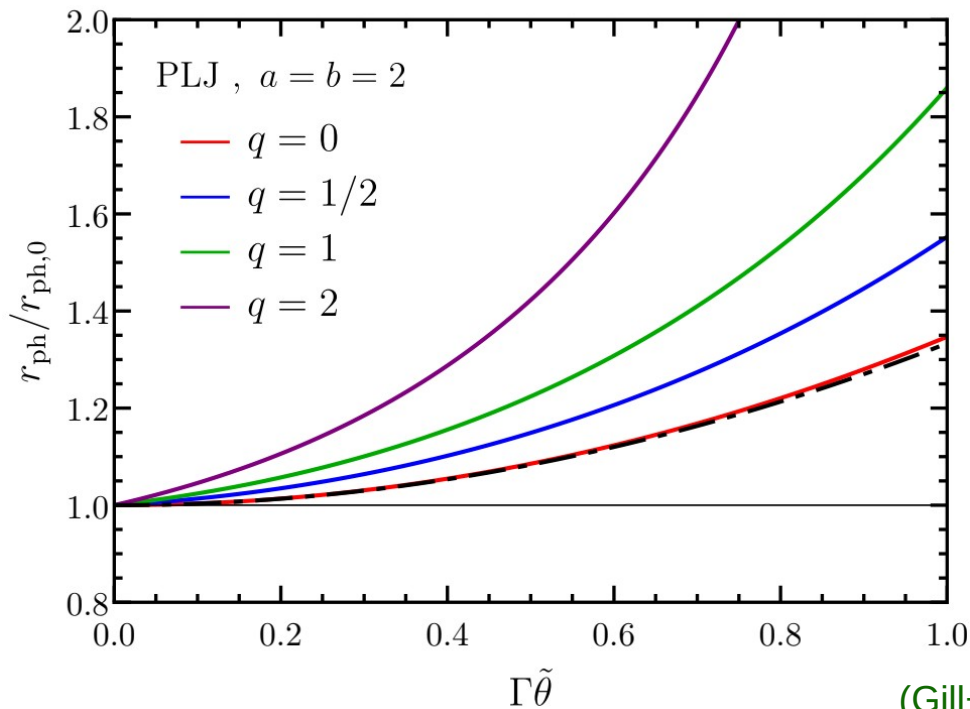
- We solve the equations of radiative transfer for an **ultra-relativistic spherical flow** and calculate the Stoke parameters in the comoving frame (see next talk by A. Beloborodov):

$$I'(r_{\text{ph}}, \mu) \quad \text{and} \quad Q'(r_{\text{ph}}, \mu) \quad 1 = \tau_T(r_{\text{ph}}) = \int_{r_{\text{ph}}}^{\infty} n'_e(r) \sigma_T \Gamma(1 - \beta) dr$$

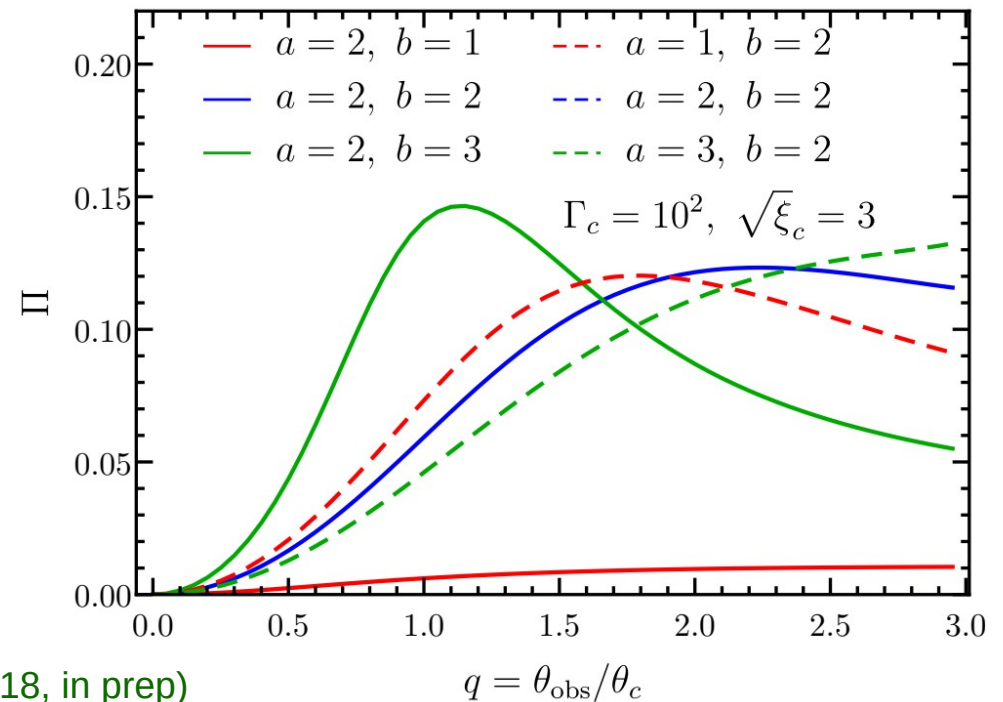
- From the comoving quantities, we calculate the total and polarized flux:

$$\Pi = \frac{Q}{I} = \frac{\int \delta_D^4 Q'(r_{\text{ph}}, \mu) dS_{\perp}}{\int \delta_D^4 I'(r_{\text{ph}}, \mu) dS_{\perp}}$$

dS_{\perp} = differential area on the plane of the sky

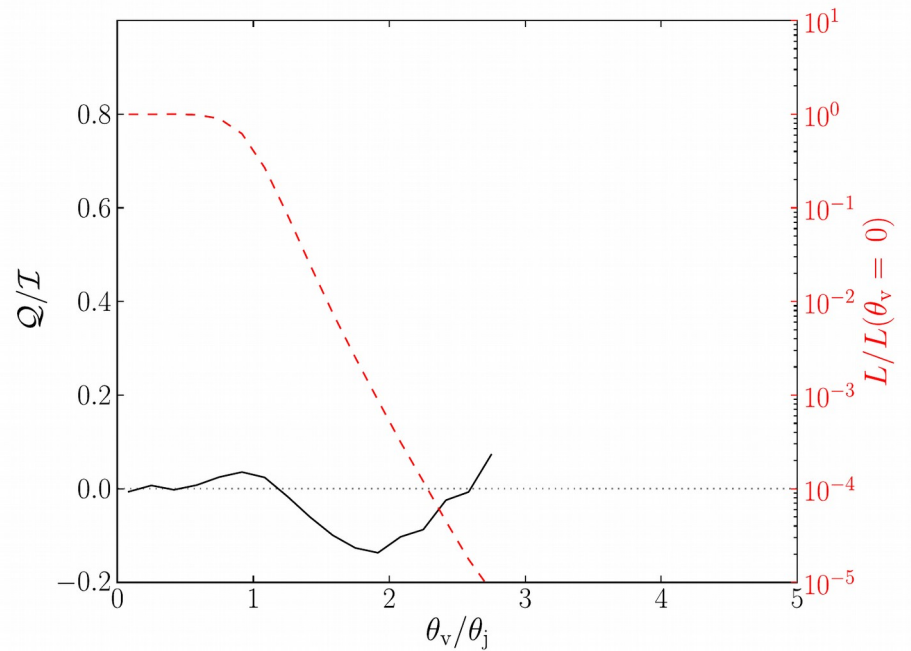
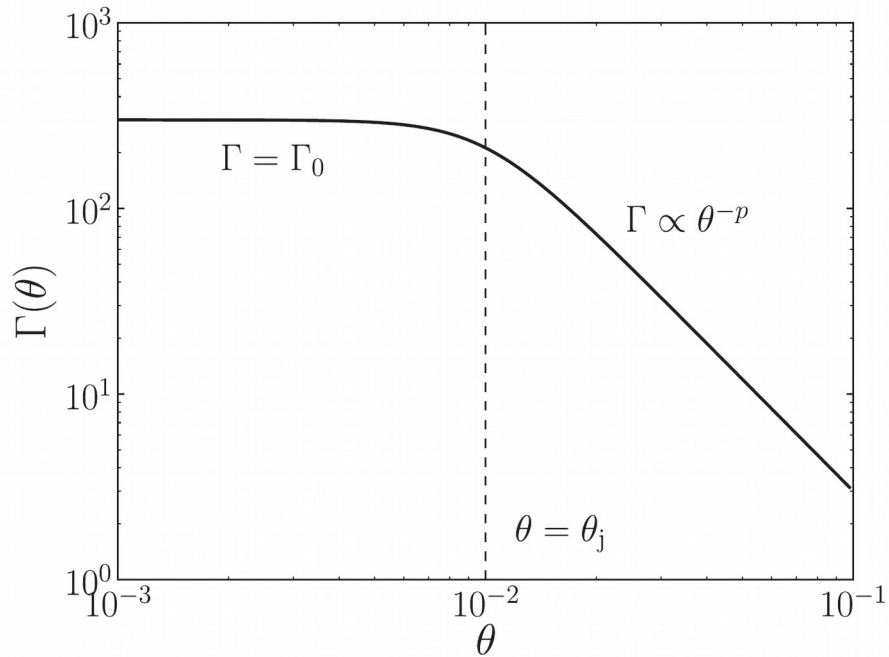


(Gill+18, in prep)



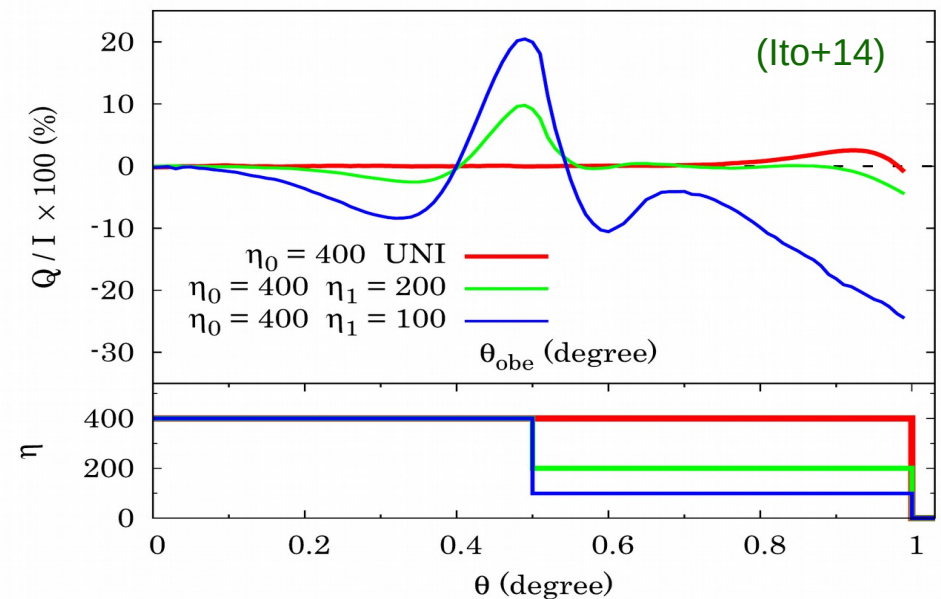
$q = \theta_{\text{obs}}/\theta_c$

Comparison with MC simulation results



(Lundman, Peer, Ryde 14)

- Both works find $\Pi \sim 10\% - 20\%$
- Also find a 90 deg change in PA



Compton drag - Polarization

- Cold electrons in the comoving frame moving at relativistic speeds with the bulk flow in the lab frame upscatter ambient soft seed photons. (**Begelman & Sikora 87**; Zdziarski+91; Shemi 94; Lazzati+00; Ghisellini+00)

$$E_{\text{scatt}} \sim \Gamma^2 E_{\text{seed}}$$

- Source of soft seed photons can be the radiation field from the exploding star in a long GRB or radiation from the walls of the funnel in which the relativistic jet propagates.

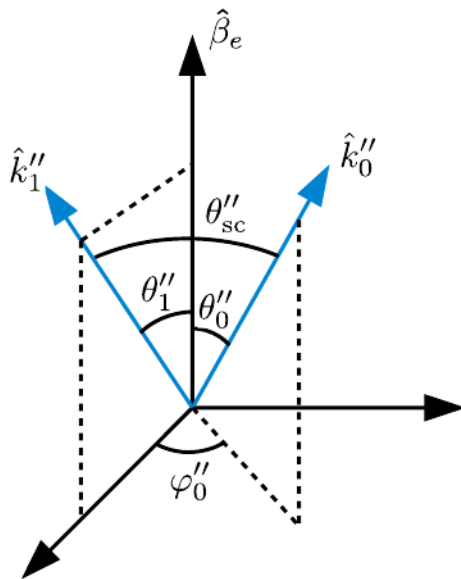
Compton drag - Polarization

- Cold electrons in the comoving frame moving at relativistic speeds with the bulk flow in the lab frame upscatter ambient soft seed photons. (Begelman & Sikora 87; Zdziarski+91; Shemi 94; Lazzati+00; Ghisellini+00)

$$E_{\text{scatt}} \sim \Gamma^2 E_{\text{seed}}$$

- Source of soft seed photons can be the radiation field from the exploding star in a long GRB or radiation from the walls of the funnel in which the relativistic jet propagates.

Polarized emission from inverse Compton scattering by cold relativistic electrons



- The degree of polarization of the scattered photon is:

$$\Pi_{\text{max}} = \frac{1 - \cos^2 \theta_{sc}''}{1 + \cos^2 \theta_{sc}''}$$

- In comparison to synchrotron emission, $0 \leq \Pi_{\text{max}} \leq 1$

Compton drag - Polarization

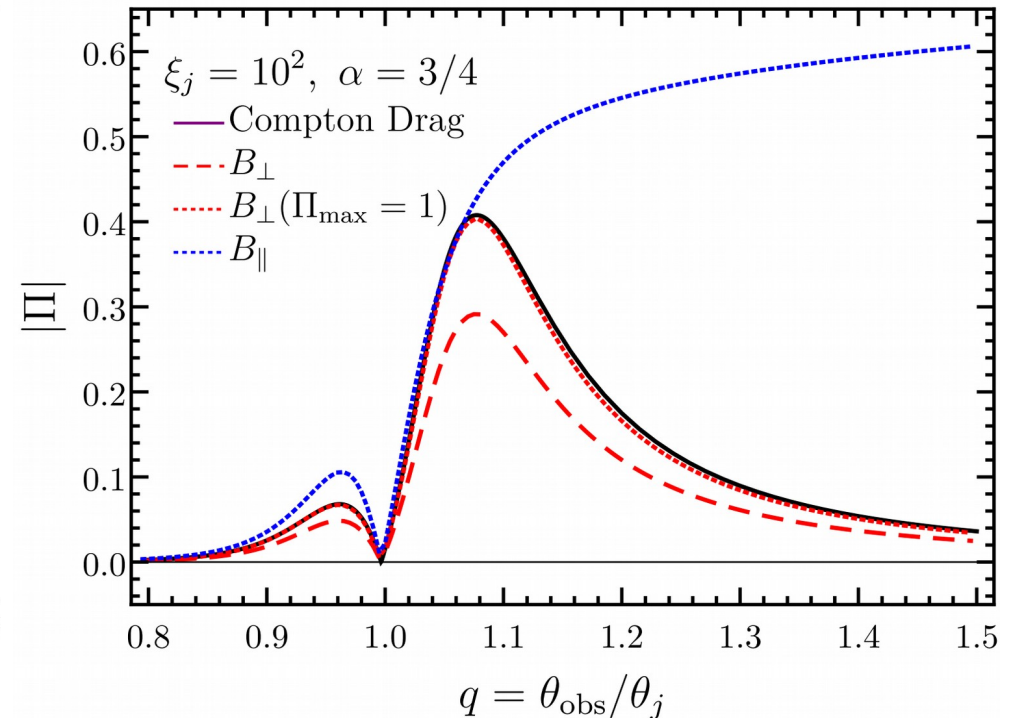
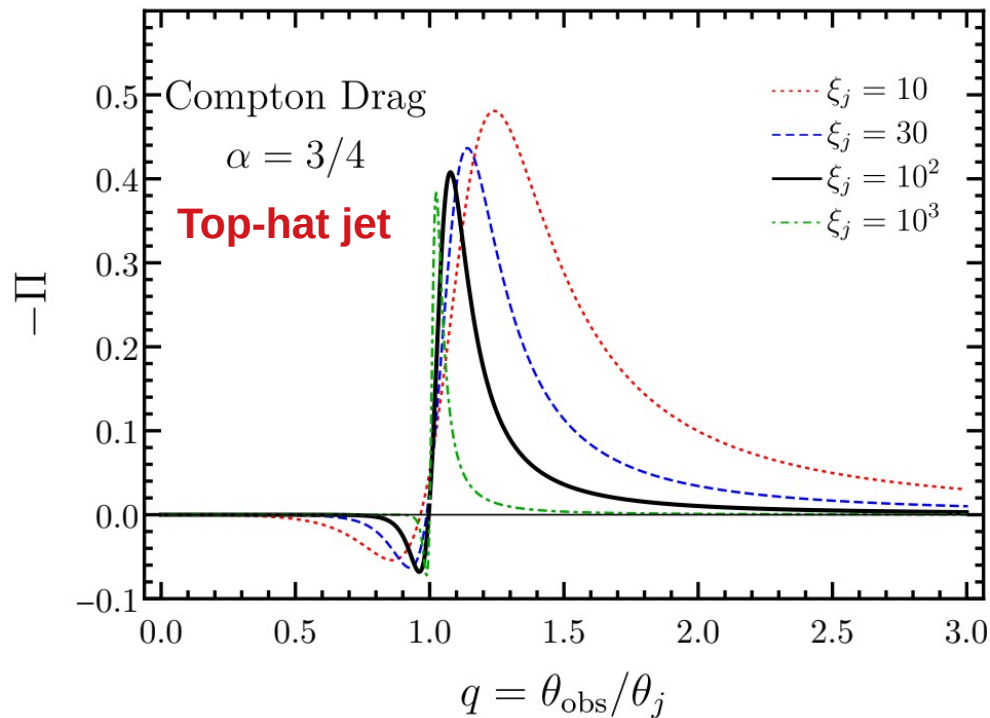
- Cold electrons in the comoving frame moving at relativistic speeds with the bulk flow in the lab frame upscatter ambient soft seed photons. (Begelman & Sikora 87; Zdziarski+91; Shemi 94; Lazzati+00; Ghisellini+00)

$$E_{\text{scatt}} \sim \Gamma^2 E_{\text{seed}}$$

- Source of soft seed photons can be the radiation field from the exploding star in a long GRB or radiation from the walls of the funnel in which the relativistic jet propagates.

Polarized emission from inverse Compton scattering by cold relativistic electrons

(Lazzati+04, Toma+09, Gill+18 in prep.)



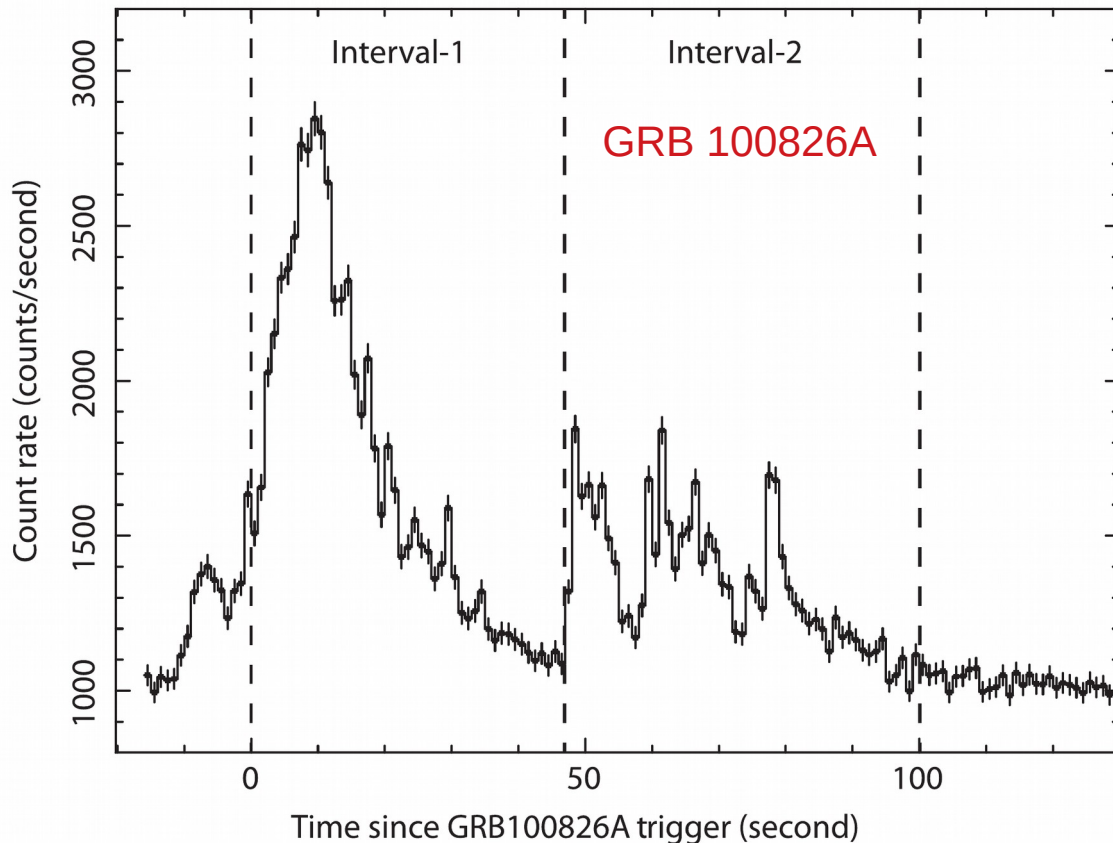
Integration over multiple pulses

Contribution of multiple pulses to an emission episode

- GRB emission is highly variable and multiple pulses contribute to each emission episode.
- The degree of polarization can vary from pulse to pulse, where the net polarization is obtained from the following for N_p number of pulses

$$\Pi = \frac{\sum_{i=1}^{N_p} Q_i}{\sum_{i=1}^{N_p} I_i}$$

(Yonetoku+11)

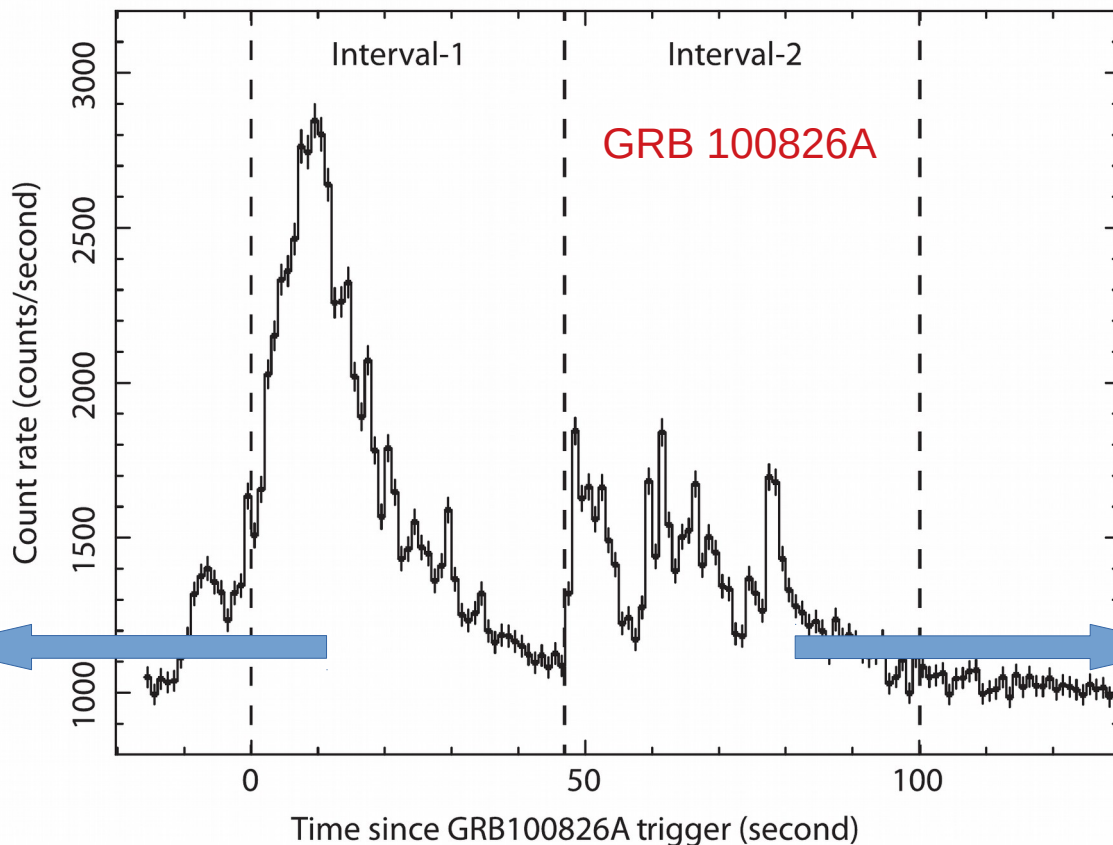


Contribution of multiple pulses to an emission episode

- GRB emission is highly variable and multiple pulses contribute to each emission episode.
- The degree of polarization can vary from pulse to pulse, where the net polarization is obtained from the following for N_p number of pulses

$$\Pi = \frac{\sum_{i=1}^{N_p} Q_i}{\sum_{i=1}^{N_p} I_i}$$

(Yonetoku+11)



$$\Pi = 0.25 \pm 0.15$$
$$\theta_p = 159^\circ \pm 18^\circ$$

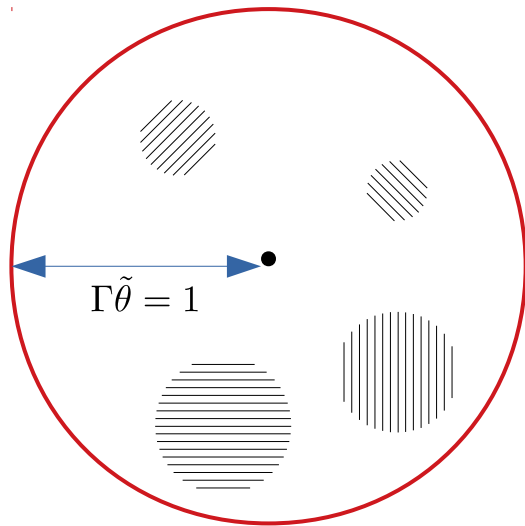
$$\Pi = 0.31 \pm 0.21$$
$$\theta_p = 75^\circ \pm 20^\circ$$

Contribution of multiple pulses to an emission episode

- GRB emission is highly variable and multiple pulses contribute to each emission episode.
- The degree of polarization can vary from pulse to pulse, where the net polarization is obtained from the following for N_p number of pulses

$$\Pi = \frac{\sum_{i=1}^{N_p} Q_i}{\sum_{i=1}^{N_p} I_i}$$

Synchrotron emission from multiple incoherent patches



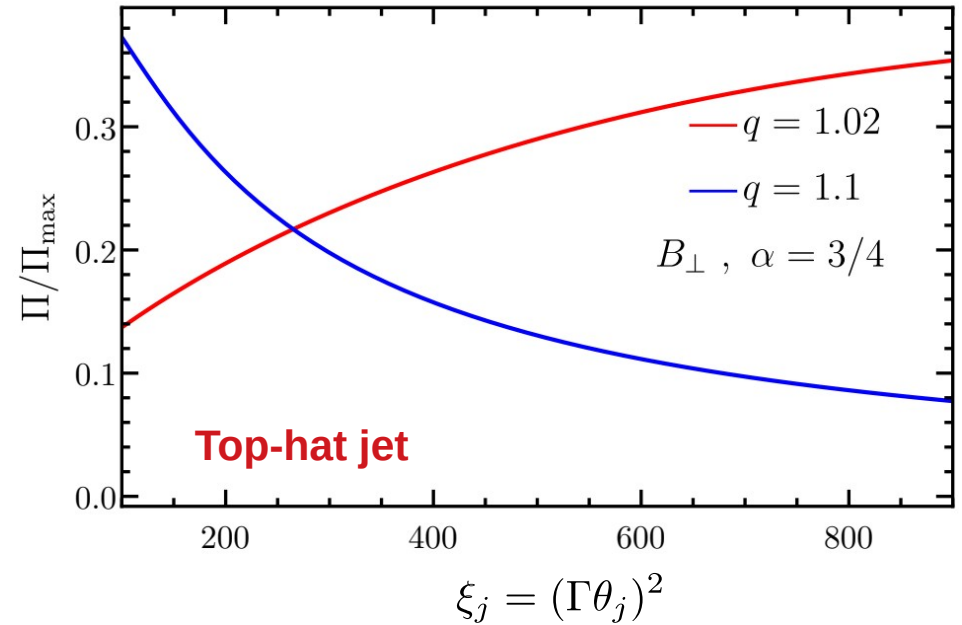
- Consider emission from multiple patches with magnetic field coherence length as large as the size of the patch
- The net polarization will be reduced to (Gruzinov & Waxman 03 – showed for afterglow polarization)

$$\Pi \sim \frac{\Pi_{\max}}{\sqrt{N_p}}$$

- Also, the PA will fluctuate from pulse to pulse

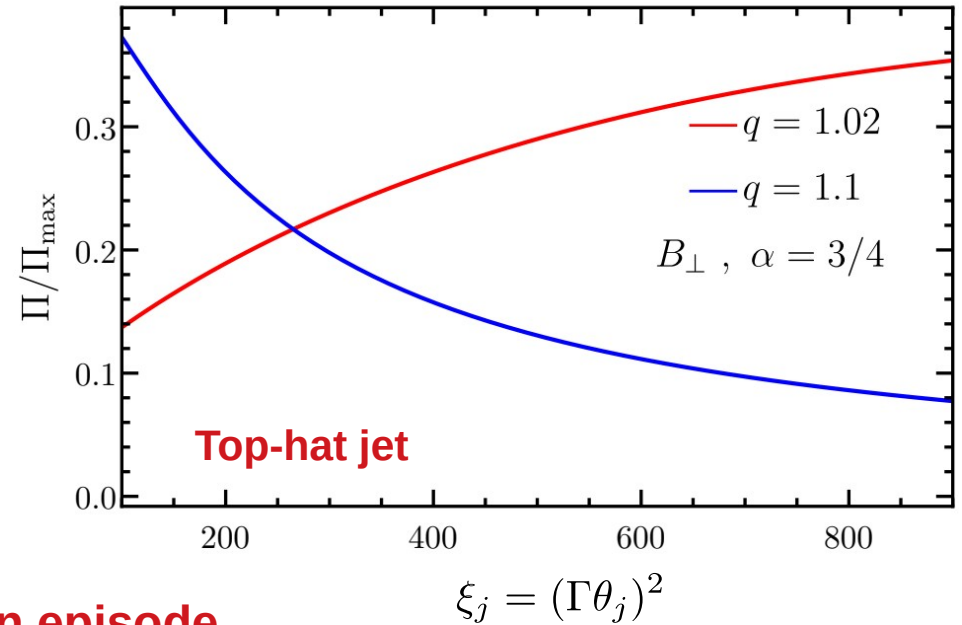
Variation of Γ and/or θ_j over multiple pulses

- It is possible that Γ and/or θ_j fluctuates between multiple pulses.
- This would effectively change ξ_j , which can reduce the net polarization upon integration over multiple pulses due to cancellation.
- This, however, requires a special LOS for a top-hat jet geometry.

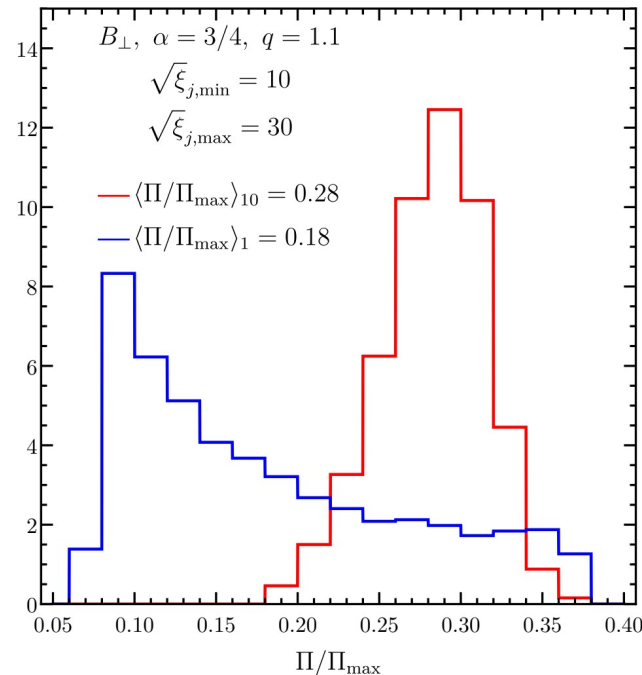
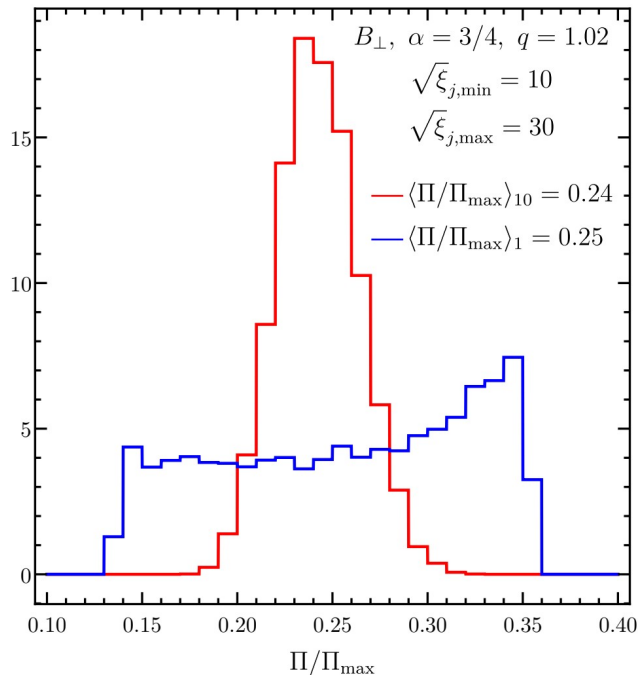


Variation of Γ and/or θ_j over multiple pulses

- It is possible that Γ and/or θ_j fluctuates between multiple pulses.
- This would effectively change ξ_j , which can reduce the net polarization upon integration over multiple pulses due to cancellation.
- This, however, requires a special LOS for a top-hat jet geometry.



MC simulations of a single emission episode



(Gill+18, in prep.)

Monte Carlo simulations of a large sample of GRBs

Monte Carlo simulations of a large sample of GRBs

- To determine the most likely level of linear polarization from different radiation processes.
- Take into account different jet structures and fluence suppression for off-axis observers.
- Integrate over multiple pulses in an emission episode with different pulses having different ξ_j

Distribution of ξ_j and q

Three basic quantities can affect Π

1) For a fixed $\theta_{\{j,c\}}$, variations in Γ can change

$$\sqrt{\xi_{\{j,c\}}} = \Gamma \theta_{\{j,c\}}$$

- We consider three distributions:

$$P(\sqrt{\xi_j}) = (\sqrt{\xi_{j,\max}} - \sqrt{\xi_{j,\min}})^{-1}$$

- Also uniform in $\ln \sqrt{\xi_j}$ and a log-normal distribution.

Distribution of ξ_j and q

Three basic quantities can affect Π

1) For a fixed $\theta_{\{j,c\}}$, variations in Γ can change

$$\sqrt{\xi_{\{j,c\}}} = \Gamma \theta_{\{j,c\}}$$

- We consider three distributions:

$$P(\sqrt{\xi_j}) = (\sqrt{\xi_{j,\max}} - \sqrt{\xi_{j,\min}})^{-1}$$

- Also uniform in $\ln \sqrt{\xi_j}$ and a log-normal distribution.

2) Distribution of viewing angle, which follows that of the solid angle:

$$P(\theta_{\text{obs}}) = \sin \theta_{\text{obs}}$$

$$\Rightarrow P(q) = \theta_j P(\theta_{\text{obs}}) \propto q$$

Distribution of ξ_j and q

Three basic quantities can affect Π

1) For a fixed $\theta_{\{j,c\}}$, variations in Γ can change

$$\sqrt{\xi_{\{j,c\}}} = \Gamma \theta_{\{j,c\}}$$

- We consider three distributions:

$$P(\sqrt{\xi_j}) = (\sqrt{\xi_{j,\max}} - \sqrt{\xi_{j,\min}})^{-1}$$

- Also uniform in $\ln \sqrt{\xi_j}$ and a log-normal distribution.

2) Distribution of viewing angle, which follows that of the solid angle:

$$P(\theta_{\text{obs}}) = \sin \theta_{\text{obs}}$$

$$\Rightarrow P(q) = \theta_j P(\theta_{\text{obs}}) \propto q$$

3) Distribution of fluence marginalized over the dist. of ξ_j :

$$\bar{f}_{\text{iso}}(q) = \int_{\xi_{j,\min}}^{\xi_{j,\max}} \tilde{f}_{\text{iso}}(q, \xi_j) P(\xi_j) d\xi_j$$

Distribution of ξ_j and q

Three basic quantities can affect Π

1) For a fixed $\theta_{\{j,c\}}$, variations in Γ can change

$$\sqrt{\xi_{\{j,c\}}} = \Gamma \theta_{\{j,c\}}$$

- We consider three distributions:

$$P(\sqrt{\xi_j}) = (\sqrt{\xi_{j,\max}} - \sqrt{\xi_{j,\min}})^{-1}$$

- Also uniform in $\ln \sqrt{\xi_j}$ and a log-normal distribution.

2) Distribution of viewing angle, which follows that of the solid angle:

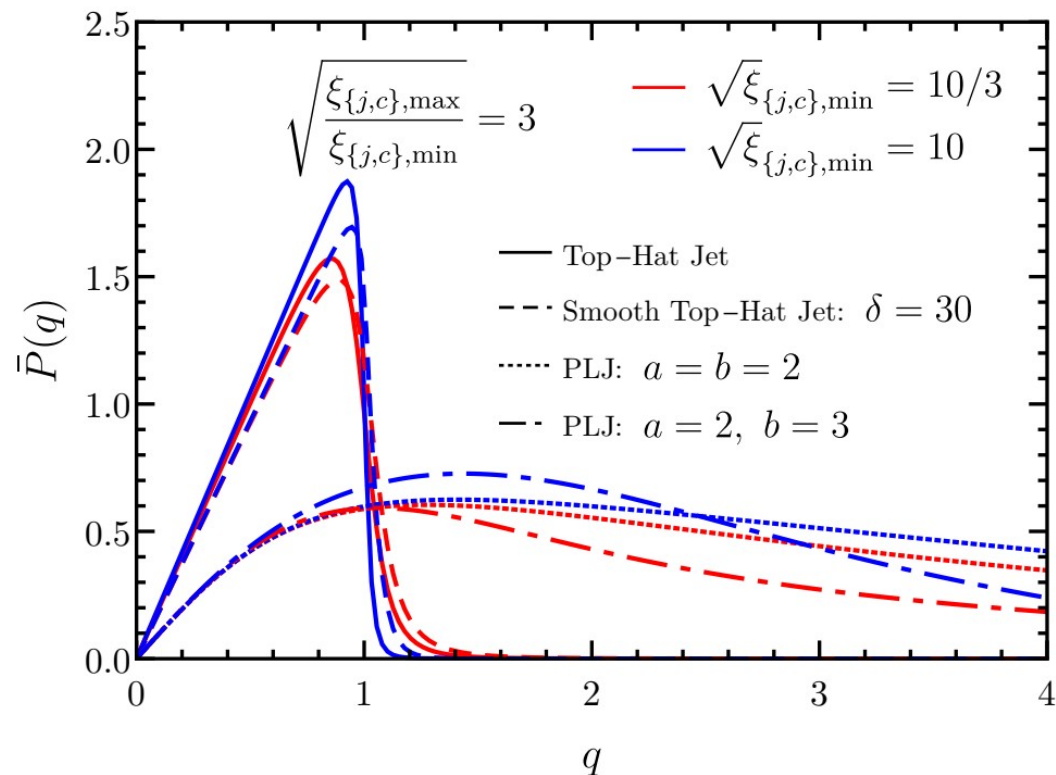
$$P(\theta_{\text{obs}}) = \sin \theta_{\text{obs}}$$

$$\Rightarrow P(q) = \theta_j P(\theta_{\text{obs}}) \propto q$$

3) Distribution of fluence marginalized over the dist. of ξ_j :

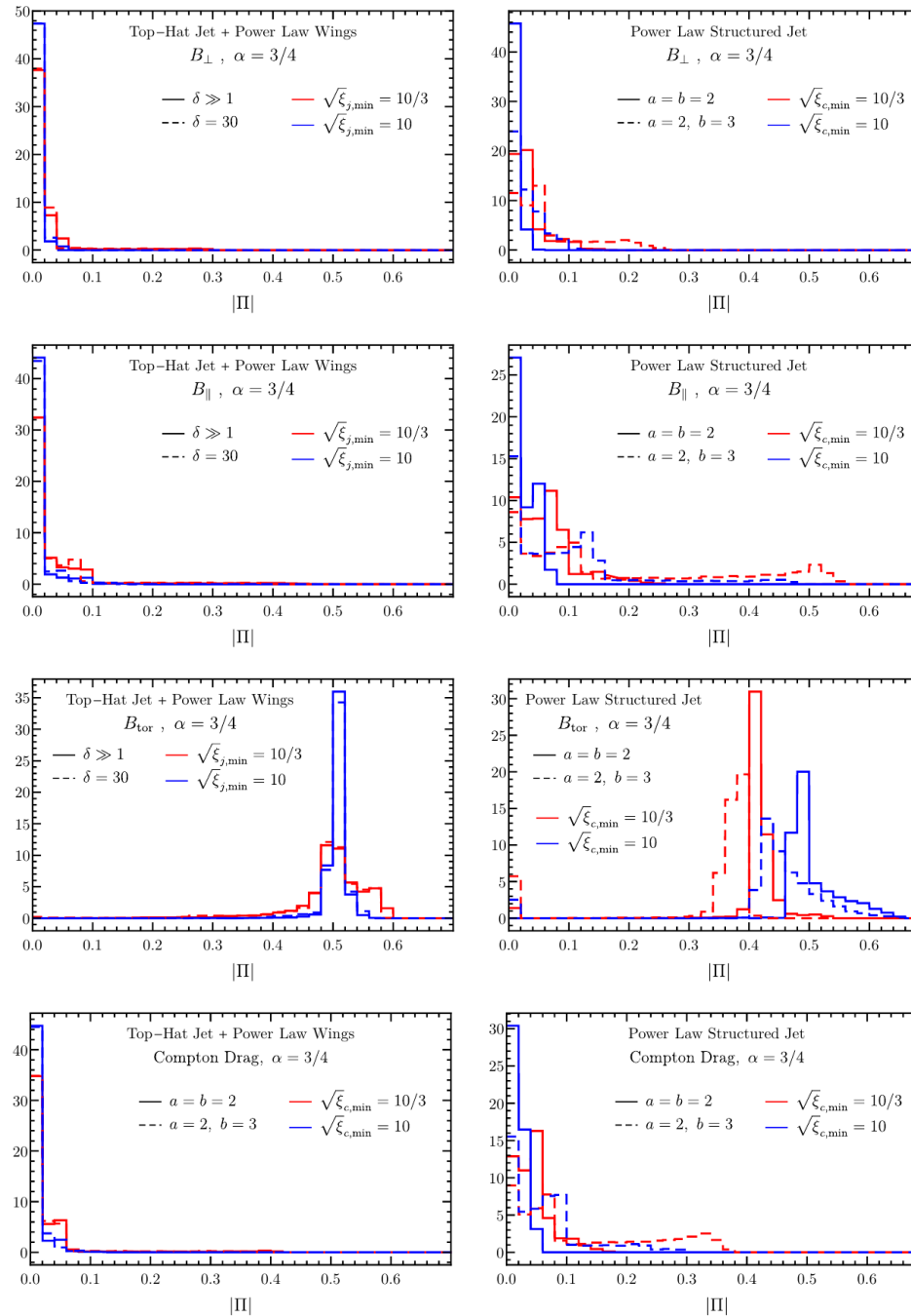
$$\bar{f}_{\text{iso}}(q) = \int_{\xi_{j,\min}}^{\xi_{j,\max}} \tilde{f}_{\text{iso}}(q, \xi_j) P(\xi_j) d\xi_j$$

(Gill+18, in prep.)



Results from Monte Carlo modeling

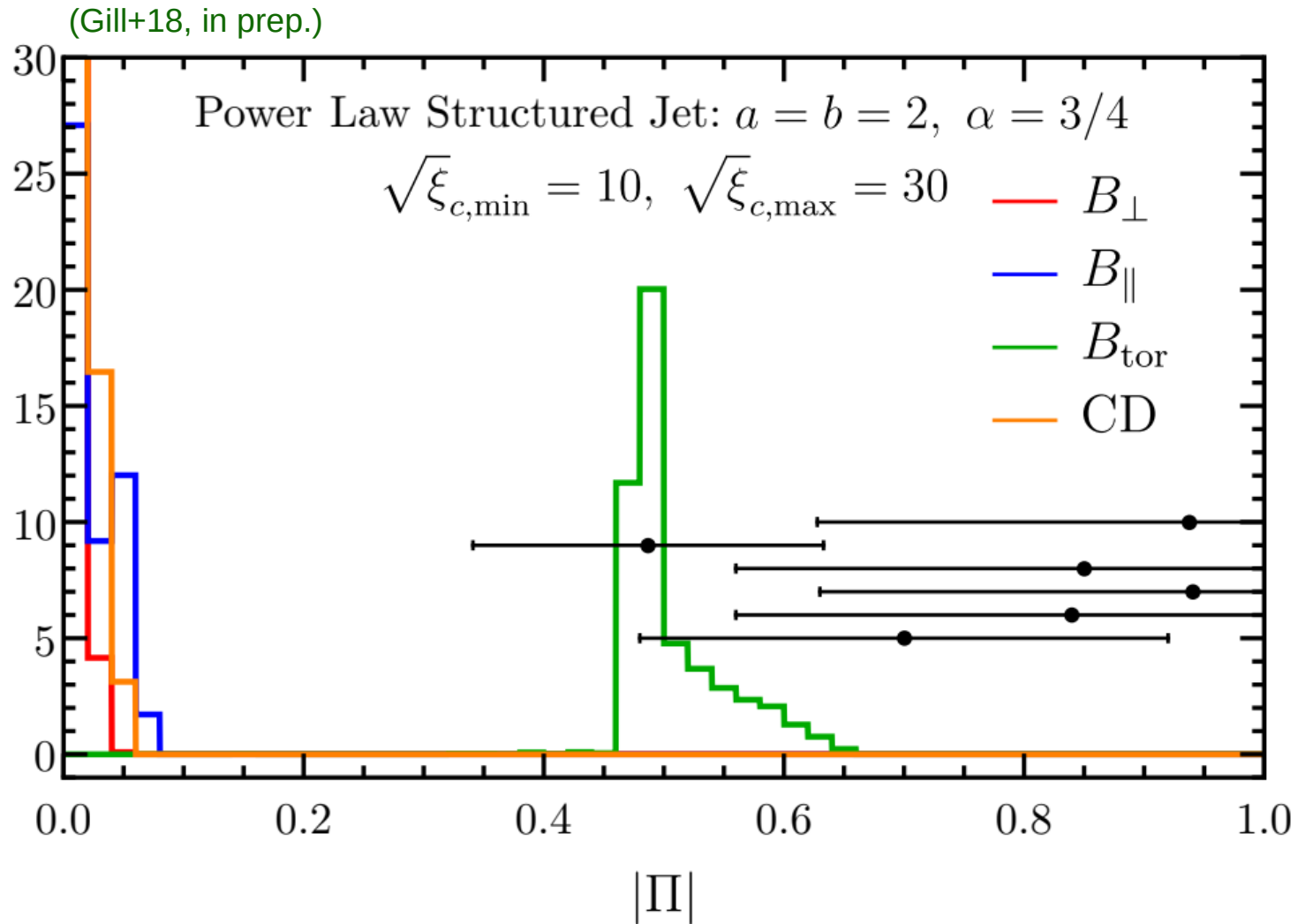
(Gill+18, in prep.)



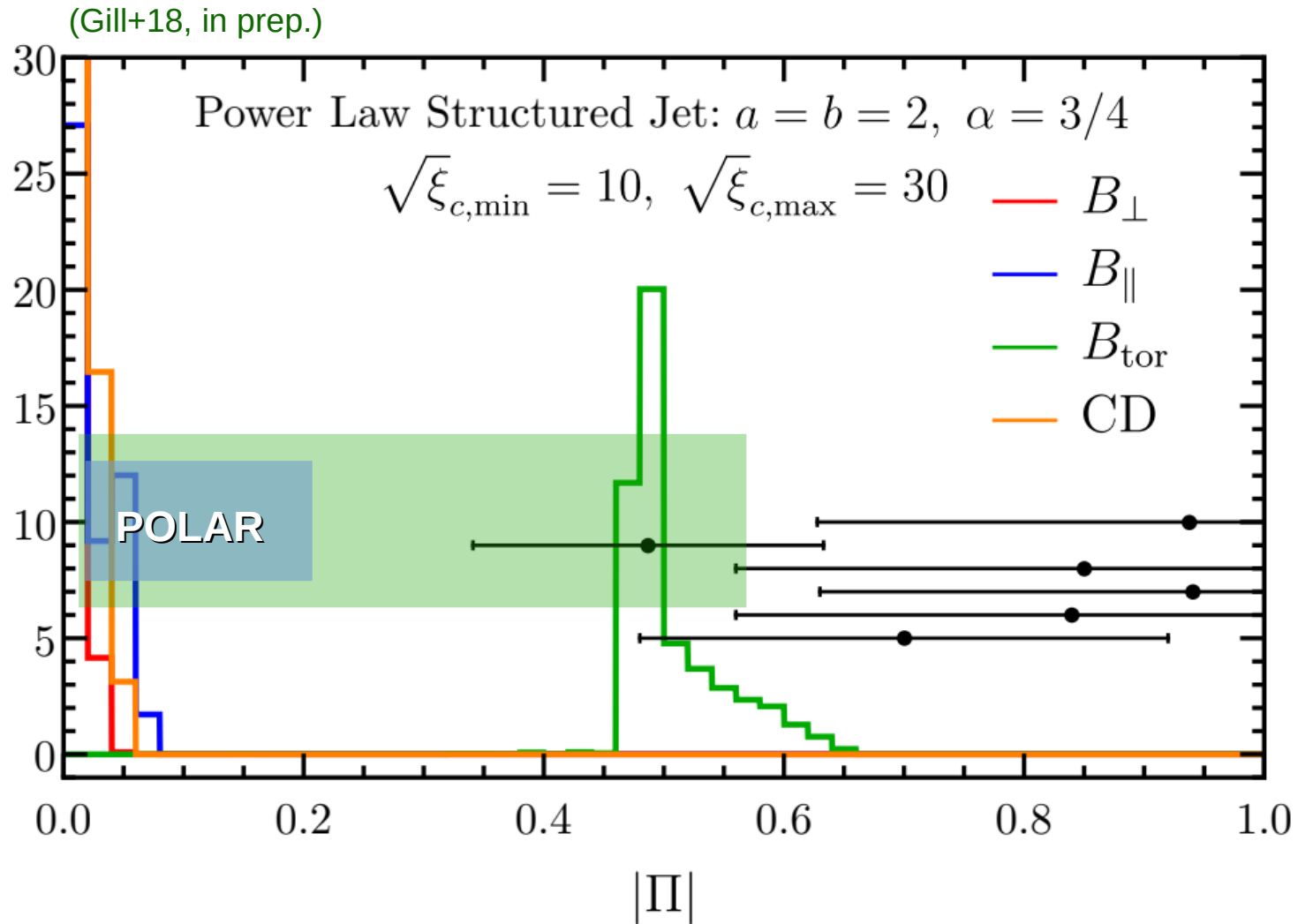
Observations of polarized prompt emission

GRB	Π (%)	PA ($^\circ$)	σ_{det} ($\Pi > 0\%$)	Instrument	Ref.
021206	80 ± 20 0 41^{+57}_{-44}	-	> 5.7 - -	<i>RHESSI</i> ^d	Coburn & Boggs (2003) Rutledge & Fox (2004) Wigger et al. (2004)
041219A	98 ± 33 63^{+31a}_{-30} 43 ± 25^b	70^{+14}_{-11} 38 ± 16	~ 2.3 ~ 2 < 2	<i>INTEGRAL-SPI</i> ^e <i>INTEGRAL-IBIS</i>	Kalemci et al. (2007) McGlynn et al. (2007) Götz et al. (2009)
100826A	27 ± 11^c	$159 \pm 18, 75 \pm 20$	2.9	<i>IKAROS-GAP</i>	Yonetoku et al. (2011b)
110301A	70 ± 22	73 ± 11	3.7	<i>IKAROS-GAP</i>	Yonetoku et al. (2012)
110721A	84^{+16}_{-28}	160 ± 11	3.3	<i>IKAROS-GAP</i>	Yonetoku et al. (2012)
160106A	68.5 ± 24	-22.5 ± 12	< 2	<i>AstroSat-CZTI</i>	Chattopadhyay et al. (2017)
160131A	94 ± 31	41.2 ± 5.0	≥ 3	<i>AstroSat-CZTI</i>	Chattopadhyay et al. (2017)
160325A	58.75 ± 23.5	10.9 ± 17	< 2	<i>AstroSat-CZTI</i>	Chattopadhyay et al. (2017)
160509A	96 ± 40	-28.6 ± 11.0	~ 2.5	<i>AstroSat-CZTI</i>	Chattopadhyay et al. (2017)
160802A	85 ± 29	-36.1 ± 4.6	≥ 3	<i>AstroSat-CZTI</i>	Chattopadhyay et al. (2017)
160821A	48.7 ± 14.6	-34.0 ± 5.0	≥ 3	<i>AstroSat-CZTI</i>	Chattopadhyay et al. (2017)
160910A	93.7 ± 30.92	43.5 ± 4.0	≥ 3	<i>AstroSat-CZTI</i>	Chattopadhyay et al. (2017)
160802A	85 ± 29	~ -32	$\sim 3(?)$	<i>AstroSat-CZTI</i>	Chand et al. (2018a)
171010A	~ 40	variable (?)	(?)	<i>AstroSat-CZTI</i>	Chand et al. (2018b)

Comparison with current measurements



Comparison with current measurements



Conclusions

- Synchrotron emission from B_{\perp} and B_{\parallel} , and from Compton drag, can yield high polarization but require a special viewing angle in the case of a top-hat jet.
 - For the case of B_{\perp} : $25\% \lesssim \Pi \lesssim 45\%$
- Non-dissipative photospheric emission requires large gradients in $\Gamma(\theta)$ to produce detectable polarization.
 - We find that $\Pi \lesssim 15\%$
- Only synchrotron emission from a large scale ordered field (like a toroidal field) can yield high levels of polarization.
 - Can get polarization as high as $50\% \lesssim \Pi \lesssim 65\%$
 - This model will also be favoured if most GRBs have $\Pi \gtrsim 20\%$
- If only $\sim 10\%$ of GRBs have $\Pi \gtrsim 20\%$ and the rest are weakly polarized then:
 - Large scale ordered fields (e.g. toroidal field) will be disfavored
 - It would mean that the structure of the jet is very close to that of a top-hat jet.

Conclusions

- Synchrotron emission from B_{\perp} and B_{\parallel} , and from Compton drag, can yield high polarization but require a special viewing angle in the case of a top-hat jet.
 - For the case of B_{\perp} : $25\% \lesssim \Pi \lesssim 45\%$
- Non-dissipative photospheric emission requires large gradients in $\Gamma(\theta)$ to produce detectable polarization.
 - We find that $\Pi \lesssim 15\%$
- Only synchrotron emission from a large scale ordered field (like a toroidal field) can yield high levels of polarization.
 - Can get polarization as high as $50\% \lesssim \Pi \lesssim 65\%$
 - This model will also be favoured if most GRBs have $\Pi \gtrsim 20\%$
- If only $\sim 10\%$ of GRBs have $\Pi \gtrsim 20\%$ and the rest are weakly polarized then:
 - Large scale ordered fields (e.g. toroidal field) will be disfavored
 - It would mean that the structure of the jet is very close to that of a top-hat jet.

Thanks!